Int. J. Heat Mass Transfer. Vol. 36, No. 5, pp. 1357–1365, 1993
Printed in Great Britain

0017–9310/93 $6.00 + 0.00

Dispersion in heat and mass transfer natural convection along vertical boundaries in porous media

RUBENS SILVA TELLES and OSVAIR V. TREVISAN
Faculdade de Engenharia Mecanica, Universidade Estadual de Campinas, 13081 Campinas-SP, Brazil

(*Received* 6 *January* 1992 *and in final form* 22 *May* 1992)

Abstract—This paper reports an analytical–numerical study on hydrodynamic dispersion in natural convection heat and mass transfer near vertical surfaces embedded in porous media. The study considers the convective flows promoted by the density variation due to the combination of temperature and concentration gradients. Scale analysis is used to determine predominant parameters from a general descriptive form for the diffusive terms in the governing equations. Four classes of flow are possible according to the relative magnitude of the dispersion coefficients. Order of magnitude reasoning is used to obtain the similarity variables and dimensionless parameters, in the search for similarity solutions. An enhanced form of the Runge–Kutta algorithm is applied to solve the system of coupled similarity equations. Results are presented for several cases in each class of flow, covering an extensive range of the governing parameters.

INTRODUCTION

THE LITERATURE on heat and mass transport in porous media points out that diffusion is proven from two basic source mechanisms with distinct phenomenology [1]. The first mechanism is that of molecular diffusion, present in almost every transport process. The drive in this mechanism is associated with the spatial gradients of the thermophysical properties. Pure heat conduction and pure mass diffusion are two classical examples of this nature. Molecular diffusion occurs in stagnant media as well as in flowing, but is the only mechanism to actuate in perfectly stagnant systems. Hydrodynamic dispersion is the second known source of diffusion. It is found in configurations of fluid moving across porous media systems. The dispersion concept helps to explain the differences often observed between transport parameters measured along and across the principal direction of fluid flow in simple geometries. Among the first fundamental work on this subject, it is worth mentioning the papers by Taylor [2] and Saffman [3]. The development of dispersion theory has been mainly related to miscible displacement and solute spreading in porous media. These areas are of major interest to secondary and tertiary oil recovery operations and to pollution control in water resources engineering.

Natural convection through porous media has received considerable attention in the last decades, partially due to the increasing demand of our society for solutions to environmental problems. The bulk of the existing work on this topic has been devoted to natural convection promoted by diffusion of a single property, temperature in most cases. Natural convection driven by the combined effects of two diffusive components is a subject of recent interest. An opportune review [4] on the topic points out that most studies have focused on the stability analysis of flows near critical conditions, therefore these are limited to the slow flow regimes that take place at the onset of the convective motion. Among the few studies concerned with the fully developed flow regimes, Bejan and Khairy [5] and more recently Lai and Kulacki [6], have addressed the problem of convection driven by double-diffusive components along a vertical plate. The present work considers the flat plate basic geometry to disclose the role played by the hydrodynamic dispersion in natural convection flows.

Hydrodynamic dispersion in porous media is modeled in the literature [1] as a tensorial quantity, with its components being either parallel or orthogonal to the main flow direction. In a comprehensive review of existing experimental work, Johnston and Perkins [7] present correlations for the longitudinal and transversal dispersion coefficients for mass transport. Longitudinal dispersion values are consistently higher than their transversal counterparts.

More recently, Hong and Tien [8] have considered the problem of natural convection in the presence of thermal dispersion along a vertical plate. The transversal component of heat dispersion was modeled as a velocity dependent term which is added to the thermal conductivity term in the energy equation. From a perturbation analysis carried on a Brinkman flow model, the authors conclude that dispersion tends to increase heat transfer while boundary and inertia effects tends to act contrarily.

The objective of the present work is to assess the effects of the hydrodynamic dispersion on the heat

NOMENCLATURE

c	similarity concentration profile
C	concentration
ΔC	concentration difference across the boundary layer
d	pore average diameter
D	mass diffusivity
D_S	dispersivity ratio
f	similarity streamfunction
g	gravitational acceleration
H	height of porous layer
II	unity tensor
K	permeability
Le	Lewis number
N	buoyancy ratio
Nu	Nusselt number
Pe	Peclet number
Ra	Rayleigh number
Ra_γ	dimensionless number, $Kg\beta\Delta T\gamma/\alpha\nu$
Ra_ξ	dimensionless number, $Kg\beta\Delta T\xi/D\nu$
Sh	Sherwood number
T	temperature
ΔT	temperature difference across the boundary layer
u, v	velocity components
V	velocity
x, y	cartesian coordinates.

Greek symbols

α	thermal diffusivity
β	thermal expansion coefficient
β_C	concentration expansion coefficient
γ	mass dispersivity, $\varepsilon_{2C}d$
δ	boundary layer thickness
ε_1	longitudinal dispersion coefficient
ε_2	transversal dispersion coefficient
η	similarity variable
θ	similarity temperature profile
ν	kinematic viscosity
ξ	thermal dispersivity, $\varepsilon_{2T}d$
ρ	density
ψ	streamfunction.

Subscripts and superscripts

$(\ )_C$	solutal properties or parameters
$(\ )_T$	thermal properties or parameters
$(\ )^*$	dimensionless variables
$(\underline{\ })$	tensor notation
$(\vec{\ })$	vector notation.

and mass transfer that occurs in natural convection flows. The focus is on the boundary layer regime promoted by the combined events of concentration and temperature gradients near a vertical wall. The study departs from the complete form of the governing equations to develop the reduced form via scale reasoning. Scale analysis is also used to sort out the possible cases according to the most important relations between the physical parameters involved. The differential equations for the various cases are then treated via similarity analysis. The numerical solution to each resulting coupled system of ordinary differential equations is obtained by an enhanced form of the Runge–Kutta algorithm. An extensive sequence of results is presented for a wide range of the main governing non-dimensional numbers.

MATHEMATICAL FORMULATION

The natural convection heat and mass transfer is considered here in the steady state regime along a flat vertical surface. The surface is embedded in a homogeneous and isotropic porous medium. The complete governing equations for the conservation of mass and momentum in two-dimensional porous systems are [4]

$$\frac{\delta u}{\delta x}+\frac{\delta v}{\delta y}=0 \tag{1}$$

$$\frac{\delta v}{\delta x}-\frac{\delta u}{\delta y}=-\frac{gK}{\nu}\left(\beta\frac{\delta T}{\delta x}+\beta_C\frac{\delta C}{\delta x}\right). \tag{2}$$

In the above equations, the Boussinesq–incompressible model has been implicitly assumed as valid to account for the density variations in the buoyancy term.

Particular attention is given in this work to the transport of energy and the chemical constituent. The dispersion mechanism is considered in the diffusion processes of both thermal energy and chemical species. Assuming local thermal equilibrium as well as the absence of chemical reaction, the conservation equations for energy and constituent are

$$u\frac{\delta T}{\delta x}+v\frac{\delta T}{\delta y}=\vec{\nabla}\cdot(\underline{\alpha}\vec{\nabla}T) \tag{3}$$

$$u\frac{\delta C}{\delta x}+v\frac{\delta C}{\delta y}=\vec{\nabla}\cdot(\underline{D}\vec{\nabla}C). \tag{4}$$

In order to maintain the original form assumed to describe diffusion and dispersion in the model, the right-hand sides of equations (3) and (4) were kept in the general vectorial notation. The coefficients $\underline{\alpha}$ and $\underline{D}$ representing the thermal and the mass overall diffusivity, respectively, have embodied in them the contributions of both molecular diffusion and hydrodynamic dispersion. In a broad view, these quantities are tensors and can be described in a general form as [9]

$$(\underline{\underline{\alpha}}; \underline{\underline{D}}) = (\alpha; D)\,[1 + (\varepsilon_{2T}^*; \varepsilon_{2C}^*)|\vec{V}^*|^2 \mathrm{II} + \{(\varepsilon_{1T}^*; \varepsilon_{1C}^*) - (\varepsilon_{2T}^*; \varepsilon_{2C}^*)\}\vec{V}^*\vec{V}^*] \quad (5)$$

where $(\underline{\underline{\alpha}}, \underline{\underline{D}})$ is the diffusivity tensor, ε_1 and ε_2 represent the longitudinal and the transversal dispersion coefficients, respectively. Subscript T refers to thermal dispersion while subscript C indicates chemical dispersion. Experimental observations [9] have indicated the dispersion coefficients as practically constant at low Peclet number regimes. In the high Peclet number range these parameters vary inversely with Peclet, or in other words, inversely with the fluid velocity. After detailing the terms in the matricial notation of equation (5), and returning all variables to the original dimensional form, the energy conservation equation can be written as

$$u\frac{\delta T}{\delta x} + v\frac{\delta T}{\delta y} = \frac{\delta}{\delta x}\left[\left(\alpha + \frac{\varepsilon_{2T}^* d^2 v^2}{\alpha} + \frac{\varepsilon_{1T}^* d^2 u^2}{\alpha}\right)\frac{\delta T}{\delta x} + \frac{(\varepsilon_{1T}^* - \varepsilon_{2T}^*)}{\alpha} d^2 uv \frac{\delta T}{\delta y}\right] + \frac{\delta}{\delta y}\left[\left(\alpha + \frac{\varepsilon_{1T}^* d^2 u^2}{\alpha} + \frac{\varepsilon_{2T}^* d^2 v^2}{\alpha}\right)\frac{\delta T}{\delta x} + \frac{(\varepsilon_{1T}^* - \varepsilon_{2T}^*)}{\alpha} d^2 uv \frac{\delta T}{\delta y}\right]. \quad (6)$$

To recast the above equations into the dimensional form, the appropriate set of non-dimensional variables was used as defined in ref. [9]. The many terms appearing on the right-hand side of equation (6) were derived via pure algebraic manipulation. The contribution of each term to the overall transfer may vary and will certainly be different for different flow configurations. The terms can be sorted out by contribution through order of magnitude analysis, after the basic scales that characterize the flow in a certain geometry have been identified. In what follows, we outline the scaling arguments concerning the boundary layer regime of the natural convection flow in the vicinity of a vertical boundary. We will refer to flow regimes of high Peclet numbers. In these regimes the dispersion coefficients are known to vary inversely with the velocity modulus, or with the Peclet number as mentioned earlier. Similar analysis can be carried out for regimes in the low Peclet range.

According to the boundary layer theory, the fluid flow taking place at the near boundary region presents scales such as

$$\frac{u}{v} \sim \frac{\delta}{H} \ll 1. \quad (7)$$

Before proceeding with the analysis, it is convenient to modify the dispersion coefficients to explicitly account for their velocity dependence

$$(\varepsilon_{1T}^*; \varepsilon_{2T}^*) = \frac{(\varepsilon_{1T}; \varepsilon_{2T})}{|\vec{V}^*|} \quad (8)$$

or

$$(\varepsilon_{1T}^*; \varepsilon_{2T}^*) = \frac{(\varepsilon_{1T}; \varepsilon_{2T})\alpha}{vd}. \quad (9)$$

Equation (9) expresses the dispersion coefficients as functions of the Peclet number, and the terms introduced in the right-hand side coincide with the definition for dispersion coefficients adopted by Johnston and Perkins [7]. As observed by these authors, the longitudinal coefficient ε_1 is higher than the transversal coefficient ε_2 in most practical cases.

After substituting equation (9) into the right-hand side of equation (6), the scales to the latter terms are

$$\frac{1}{\delta}\left[\left(\alpha; \varepsilon_{2T} dv; \varepsilon_{1T} d\frac{u^2}{v}\right)\frac{\Delta T}{\delta}; \varepsilon_{1T} ud\frac{\Delta T}{H}\right]$$

$$\frac{1}{H}\left[\left(\alpha; \varepsilon_{1T} dv; \varepsilon_{2T} d\frac{u^2}{v}\right)\frac{\Delta T}{\delta}; \varepsilon_{1T} ud\frac{\Delta T}{H}\right]. \quad (10)$$

Comparison between the orders of magnitude expressed in equation (10) can be straightforward if we invoke the geometric relation of the boundary layer in equation (7) and consider that although $\varepsilon_{1T} > \varepsilon_{2T}$, scales of H and δ are such that $\varepsilon_{2T}H$ is still greater than $\varepsilon_{1T}\delta$. Screening the orders sequentially, all the terms are ruled out by the first two terms in expression (10). From all the possibilities introduced by the dispersion components in the porous medium, only the cross product of the transversal coefficient and the longitudinal velocity remains as the relevant dispersive agent to diffuse energy. The energy equation can be then simplified to

$$u\frac{\delta T}{\delta x} + v\frac{\delta T}{\delta y} = \frac{\delta}{\delta x}\left[(\alpha + \varepsilon_{2T} dv)\frac{\delta T}{\delta x}\right]. \quad (11)$$

By the same reasoning used to obtain equation (11), the constituent conservation equation is reduced to

$$u\frac{\delta C}{\delta x} + v\frac{\delta C}{\delta y} = \frac{\delta}{\delta x}\left[(D + \varepsilon_{2C} dv)\frac{\delta C}{\delta x}\right]. \quad (12)$$

Both parameters $(\varepsilon_{2T}, \varepsilon_{2C})$ and d are essentially characteristic properties of the saturated porous medium. Relatively few data are available on heat dispersion, but estimates for the product $\varepsilon_{2T}d$ from published data [10] span between 10^{-5} and 10^{-3} m, for sandstone–water media. More research has been done on mass dispersion, and known values of $\varepsilon_{2C}d$ are typically one order of magnitude lower. It should be stressed though, that the lower value of the constituent dispersion coefficient does not imply a lesser influence on the combined diffusive effect. Indeed, for the common water–glucose or water–chlorine solutions, heat diffusivity is two orders of magnitude greater than mass diffusivity. In these cases, $\varepsilon_{2C}d$ has a much greater impact on diffusion of the chemical components than $\varepsilon_{2T}d$ has over heat diffusion. When considering double-diffusion phenomena, if $Le > 1$, as in the cases mentioned, the dispersive contribution of $\varepsilon_{2T}dv$

can be neglected with respect to the effects of α up to a higher range of fluid velocities.

In the next section, the variety of regimes possible under different combinations of diffusion parameters is sorted out via scale analysis. For notation simplicity, the products $\varepsilon_{2T}d$ and $\varepsilon_{2C}d$ will be referred to simply as ξ and γ, respectively.

SCALE ANALYSIS

Consider the two-dimensional region of a saturated porous medium near a vertical flat boundary. Conservation of mass and momentum are given by equations (1) and (2). The governing equations for energy and constituent, after being reduced accordingly to the boundary layer theory, are

$$u\frac{\delta T}{\delta x}+v\frac{\delta T}{\delta y}=\frac{\delta}{\delta x}\left[(\alpha+\xi v)\frac{\delta T}{\delta x}\right] \tag{13}$$

$$u\frac{\delta C}{\delta x}+v\frac{\delta C}{\delta y}=\frac{\delta}{\delta x}\left[(D+\gamma v)\frac{\delta C}{\delta x}\right]. \tag{14}$$

The scale analysis in this case can be carried out in different ways. We chose to start by examining the scales that are embodied in the energy and constituent equations. This choice is suggested by the primary interest, which is to study the role played by the dispersion coefficients. Comparing the molecular diffusion and the dispersion terms in equations (13) and (14), four different classes of problems are anticipated from the combination of possibilities

$$1-\alpha \gg \xi v \quad \text{and} \quad D \ll \gamma v$$

$$2-\alpha \gg \xi v \quad \text{and} \quad D \gg \gamma v$$

$$3-\alpha \ll \xi v \quad \text{and} \quad D \gg \gamma v$$

$$4-\alpha \ll \xi v \quad \text{and} \quad D \ll \gamma v.$$

Each of these classes will branch out new groups, when the continuity and momentum scale balances are brought into the analysis. The driving force in the momentum equation is due either to the temperature gradient or to the concentration gradient. The driving mechanism is itself used to distinguish the two flow regimes, the first called heat-transfer-driven and the last known as mass-transfer-driven. One final subdivision is proportioned by the comparison between the heat and mass diffusion properties of the flow.

Consider the first class of flow, when thermal diffusion is predominant and mass dispersion supersedes mass diffusion. The energy equation will read

$$u\frac{\delta T}{\delta x}+v\frac{\delta T}{\delta y}=\alpha\frac{\delta^2 T}{\delta x^2} \tag{15}$$

and the scales of δ_T, v and Nu depend on the relative magnitude of the terms $\beta\Delta T$ and $\beta_C\Delta C$. In situations of heat-transfer-driven flows ($\beta\Delta T \gg \beta_C\Delta C$), Nu varies as $Ra^{1/2}$. This result is the same obtained for pure heat transfer natural convection, which is a simple particular case of the double-diffusive convection with no heat dispersion and no accounting for the transport of chemical species.

The mass transfer scales can be found from the constituent conservation equation, now reading

$$u\frac{\delta C}{\delta x}+v\frac{\delta C}{\delta y}=\frac{\delta}{\delta x}\left(\gamma v\frac{\delta C}{\delta x}\right). \tag{16}$$

Integrating equation (16) across the boundary layer results in

$$\frac{\mathrm{d}}{\mathrm{d}y}\int_0^x v\Delta C\,\mathrm{d}x=-\gamma\left(v\frac{\delta C}{\delta x}\right)_{x=0}. \tag{17}$$

In scaling terms

$$\frac{v\Delta C}{H}\min(\delta_C,\delta_T)\sim\gamma\frac{\Delta C}{\delta_C}. \tag{18}$$

Here the analysis branches off again, now into subclasses where $\delta_T \gg \delta_C(\alpha \gg \gamma v)$ or $\delta_T \ll \delta_C$ $(\alpha \ll \gamma v)$. Proceeding with the $\alpha \gg \gamma v$ case from equation (18)

$$\delta_C \sim (\gamma H)^{1/2} \tag{19}$$

or

$$Sh \sim \left(\frac{\gamma}{H}\right)^{-1/2} \tag{20}$$

with Sh corresponding to the dimensionless mass transfer rate.

The scales for classes 2, 3 and 4 can be derived in an analogous procedure. Table 1 summarizes all the results relative to the first class, including the branchings mentioned but not detailed in the analysis. Table 1 also shows the validity criteria for each class, expressed in order of magnitude terms.

The results concerning the second class can be obtained by repeating the reasoning presented during the analysis of the first case, observing that all the basic equations remain unaltered except for the constituent conservation equation, which now is expressed by

$$u\frac{\delta C}{\delta x}+v\frac{\delta C}{\delta y}=D\frac{\delta^2 C}{\delta x^2}. \tag{21}$$

Along with the continuity, momentum and energy equations, equation (21) describes the class of problem where hydrodynamic dispersion is neglected in both energy and mass transport. This case has been treated in the literature [5] and the scales involved are known.

The same scheme of analysis could be used to reveal the scaling relations that are valid in the other two classes (3 and 4). An alternative way is to correlate the scales of the different cases by observing the similarities that exist across the classes. By writing the governing equations side by side for two classes at a time, the symmetry rules between the systems of equations become apparent. These rules were used to

Table 1. Scales for dispersion only in transport of chemical species

Driving mechanism	v	Nu	Sh	Criteria
Heat transfer $\lvert N\rvert \ll 1$	$\frac{\alpha}{H}Ra$	$Ra^{1/2}$	$\left(\frac{\gamma}{H}\right)^{-1} Ra^{-1/2}$	$Ra_\gamma \gg 1$
	$\frac{\alpha}{H}Ra$	$Ra^{1/2}$	$\left(\frac{\gamma}{H}\right)^{-1/2}$	$Ra_\gamma \ll 1$
Mass transfer $\lvert N\rvert \gg 1$	$\frac{\alpha}{H}Ra\lvert N\rvert$	$(Ra\lvert N\rvert)^{1/2}$	$\left(\frac{\gamma}{H}\right)^{-1/2}$	$Ra_\gamma \lvert N\rvert \gg 1$
	$\frac{\alpha}{H}Ra\lvert N\rvert$	$Ra\lvert N\rvert\left(\frac{\gamma}{H}\right)^{1/2}$	$\left(\frac{\gamma}{H}\right)^{-1/2}$	$Ra_\gamma \lvert N\rvert \ll 1$

obtain the scaling laws displayed in Table 2, for the flows of class 4.

SIMILARITY SOLUTION

The scale analysis presented in the preceding section is very useful to indicate possible self-similar relations in the differential equations. And, if it applies, to indicate which are the most proper—scaling wise—similarity transformations. Starting with the case where hydrodynamic dispersion is predominant in diffusing the chemical constituent, while the heat diffusion is primarily by conduction, the adequate variable transformation is

$$\eta_{1,2} = \frac{x}{yRa_y^{-1/2}}$$

$$f_{1,2} = \frac{\psi}{\alpha Ra_y^{1/2}}. \tag{22}$$

The ordinary equations resulting from the substitution of equation (22) into equations (1), (2), (15) and (16) are

$$f_1'' = -\theta' - NC'$$
$$\theta'' = \tfrac{1}{2} f_1 \theta'$$
$$C'' = -\frac{C'}{f_1'}\left[f_1'' + Ra_y \frac{f_1}{2}\right]. \tag{23}$$

The variables defined in equation (22) can also be used to reduce the governing equations of class 2 to the system

$$f_2'' = -\theta' - NC'$$
$$\theta'' = \tfrac{1}{2} f_2 \theta'$$
$$C'' = \tfrac{1}{2} Le f_2 C'. \tag{24}$$

For class 3, the similarity transformation chosen is

$$\eta_{3,4} = \frac{x}{(\xi y)^{1/2}}$$
$$f_{3,4} = \frac{\psi}{\left(\frac{\xi}{y}\right)^{1/2} \alpha Ra_y} \tag{25}$$

which renders the following system

$$f_3'' = -\theta' - NC'$$
$$\theta'' = -\frac{\theta'}{f_3'}\left[f_3'' + \frac{f_3}{2}\right]$$
$$C'' = \tfrac{1}{2} Ra_\xi f_3 C'. \tag{26}$$

Using the pair of variables defined in equation (25), the equations for the dispersion-governed convection of class 4 become

Table 2. Scales for dispersion in both heat and mass transfer

Driving mechanism	v	Nu	Sh	Criteria
Heat transfer $\lvert N\rvert \ll 1$	$\frac{Kg\beta\Delta T}{\nu}$	$\left(\frac{\xi}{H}\right)^{-1/2}$	$\left(\frac{\xi}{H}\right)^{1/2}\left(\frac{\gamma}{H}\right)^{-1}$	$D_S \ll 1$
	$\frac{Kg\beta\Delta T}{\nu}$	$\left(\frac{\xi}{H}\right)^{-1/2}$	$\left(\frac{\gamma}{H}\right)^{-1/2}$	$D_S \gg 1$
Mass transfer $\lvert N\rvert \gg 1$	$\frac{Kg\beta_C\Delta C}{\nu}$	$\left(\frac{\gamma}{H}\right)^{1/2}\left(\frac{\xi}{H}\right)^{-1}$	$\left(\frac{\gamma}{H}\right)^{-1/2}$	$D_S \gg 1$
	$\frac{Kg\beta_C\Delta C}{\nu}$	$\left(\frac{\xi}{H}\right)^{-1/2}$	$\left(\frac{\gamma}{H}\right)^{-1/2}$	$D_S \ll 1$

$$f''_4 = -\theta' - NC'$$

$$\theta'' = -\frac{\theta'}{f'_4}\left[f''_4 + \frac{f_4}{2}\right]$$

$$C'' = -\frac{C'}{f'_4}\left[f''_4 + D_S\frac{f_4}{2}\right] \quad (27)$$

where D_S is the ratio between the thermal and the chemical dispersion coefficients, $D_S = \xi/\gamma$.

Each of the mathematical problems posed by the sets of ordinary equations (23), (24), (26) and (27) can be solved numerically. The Runge–Kutta algorithm is known to be efficient in solving differential equations of this category. The procedure used to obtain the results presented in this paper is based on a fourth-order Runge–Kutta scheme. The initial value problem created by the boundary condition which is specified at the outer boundary can be handled by a shooting algorithm. Some difficulties may arise though, due to the coupling of the non-linear equations. At least two initial values must be guessed in the shooting process, in order to match the solution to the condition at the region far from the vertical boundary. Once the temperature and concentration are fixed at the boundary, the next closest estimate may be on the gradients of these variables. The solutions encountered by the numerical calculation depend on the values guessed for $\theta'(0)$ and $C'(0)$, i.e.

$$\theta(\infty) = \theta[\theta'(0), C'(0)] \quad (28)$$

$$C(\infty) = C[\theta'(0), C'(0)]. \quad (29)$$

Also, as solutions to boundary layer problems, the profiles must be asymptotic at positions far enough into the medium. Such restriction can be monitored by the values

$$\theta'(\infty) = \theta'[\theta'(0), C'(0)] \quad (30)$$

$$C'(\infty) = C'[\theta'(0), C'(0)]. \quad (31)$$

At stages where the final converged solution is not yet reached, the values given by equations (28)–(31) are non-zero and may be represented by residuals. The problem hereon becomes an optimization problem, where the objective is to minimize the residuals or the combination of them. The shooting procedure adopted in the present work follows the Nachtsheim–Swigert [11] method, seeking the least square sum of the residuals. Although the method provides unique, asymptotic solutions, the numerical procedure may require relaxation in order to achieve convergence. As the problems in our study frequently lead to the solution of ill-conditioned matrices, a Marquardt [12] scheme was employed to provide proper numerical relaxation whenever needed.

RESULTS

Results obtained from the numerical procedure described in the preceding section are reported for each class flow. An inter-case comparison is made for the most important characteristics as velocity, temperature and concentration profiles. Numerical values are reported in each case for the local transfer rates, in terms of local Nusselt and Sherwood numbers. Runs were organized by classes of flow, in the same sequence presented in the previous sections.

Regarding class 1 flows, the mathematical problem posed by equation (23) along with the boundary conditions was solved via integration in η from zero to values as high as 15. The increment $\Delta\eta$ used to perform the integration was 2.5×10^{-4}: this increment was found to be small enough to render solutions insensitive to further decreases in $\Delta\eta$. The results summarized in Table 3 were obtained using the shooting success criterion of 2.0×10^{-4}. In other words, the solution was considered satisfactory when the calculated values for the residuals in equations (28)–(31) were altogether smaller than 2.0×10^{-4}. Relaxation through Marquardt's algorithm was necessary to reach converged solutions in this case. In accordance with the variable transformation for cases 1 and 2, the local Nusselt and Sherwood numbers are

$$Nu = -\theta'(0)Ra_y^{1/2} \quad (32)$$

$$Sh = -C'(0)Ra_y^{1/2}. \quad (33)$$

The velocity profiles presented in Fig. 1(a) show the influence of mass dispersion on the hydrodynamic boundary layer. The trend is for the boundary layer to thicken as mass dispersion increases. The graph refers to the situation of balanced heat and mass buoyancy forces. Similar patterns are obtained for different values of $N \neq 0$ [13]. For small values of Ra_y, the velocity profiles tend to resemble the profiles obtained with $|N| \ll 1$. Figure 1(b) illustrates the temperature field near the boundary. The dispersion of constituents improves the heat transfer to the flat boundary, as the thermal boundary layer decreases with Ra_y for all cases with $N \neq 0$. As pointed out by the scale analysis this effect is more pronounced towards higher values of N. A reverse effect is observed on the species concentration distribution. Figure 1(c) shows that the constituent-rich layer thickens as the dispersion number increases. This influence on the transport of species is also seen when N is zero, a condition in which the effects of dispersion do not interfere with either the heat transfer or the fluid flow.

For the numerical solution on flows of class 2, the values used as parameters for the numerical integration of equation (24) were the same employed in the preceding problem, except for $\Delta\eta$ which was set to 2.5×10^{-3}. This problem refers to the class where hydrodynamic dispersion is totally absent. The results obtained reproduced exactly the values published earlier [5, 6] for the case of pure molecular diffusion. Runs on this problem served as validation tests for our numerical scheme.

Parameter Ra_y is expected to vary in the order of 0–10 for occurrences of natural convection in saturated

Table 3. Numerical values from the similarity solution to flows of class 1

N	Ra_γ	$Nu_\gamma Ra_\gamma^{-1/2}$	$Sh_\gamma Ra_\gamma^{-1/2}$
0	0.1	0.444	1.596
	0.5	0.444	0.618
	0.8	0.444	0.456
	1	0.444	0.393
	2	0.444	0.241
	4	0.444	0.142
	6	0.444	0.102
	9	0.444	0.072
	100	0.444	0.0078
0.1	1	0.464	0.385
0.2	1	0.484	0.379
0.5	1	0.544	0.367
0.8	1	0.604	0.360
1	0.1	0.536	1.362
	0.5	0.609	0.545
	0.8	0.632	0.410
	1	0.642	0.356
	2	0.671	0.229
	4	0.691	0.146
	6	0.698	0.112
	9	0.704	0.086
2	0.1	0.632	1.289
	0.5	0.770	0.525
	0.8	0.807	0.399
	1	0.823	0.349
	2	0.860	0.231
	4	0.882	0.154
	6	0.889	0.121
	9	0.895	0.096
3	0.1	0.730	1.255
	0.5	0.920	0.518
	0.8	0.964	0.396
	1	0.981	0.349
	2	1.019	0.235
	4	1.040	0.160
	6	1.048	0.128
	9	1.054	0.102
4	0.1	0.828	1.235
	0.5	1.059	0.514
	0.8	1.104	0.396
	1	1.121	0.350
	2	1.157	0.239
	4	1.178	0.164
	6	1.186	0.132
	9	1.192	0.106

porous media of low to medium porosity, while Ra_ξ is two orders of magnitude greater for the same configuration. The last range comprises the values used for Ra_ξ in the calculations relative to flows in class 3. Recalling the similarity transformations applied to the governing equations in this case, the local Nusselt and Sherwood numbers are now given by

$$Nu = -\theta'(0)\left(\frac{\xi}{y}\right)^{-1/2} \tag{34}$$

$$Sh = -C'(0)\left(\frac{\xi}{y}\right)^{-1/2}. \tag{35}$$

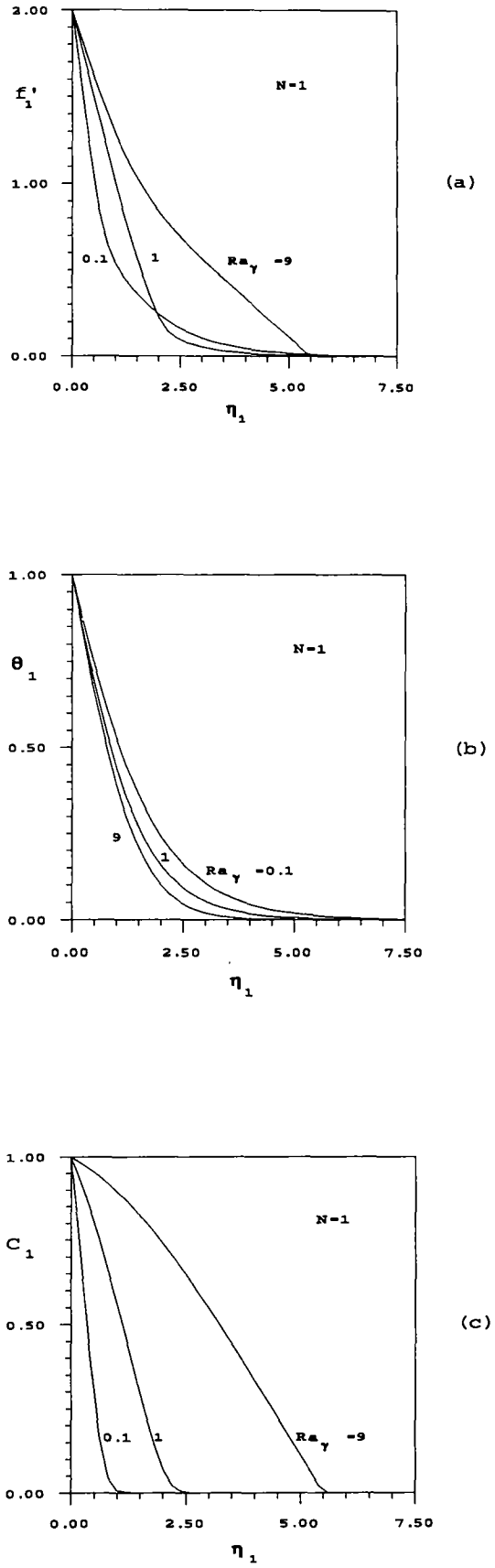

FIG. 1. Influence of chemical dispersion on (a) fluid velocity, (b) temperature profile and (c) species distribution, in class 1 flows.

Table 4 displays the results relative to the circumstances where heat diffuses primarily by dispersion. The heat transfer rate decreases with an increasing dispersion activity for this extreme case. This trend is consistent with the scaling law predicted for Nu. The velocity profile presented in Fig. 2 illustrates the effect of heat dispersion upon fluid motion close to the boundary. The same plot can be used to visualize the temperature profile, since when $N = 0$ the velocity and the temperature solutions coincide. The temperature gradient is diminished by the increased fluid mixing from hydrodynamic dispersion near the boundary. The temperature distribution is more linear than the profiles observed in pure diffusion cases. The distribution of the chemical species however, presents a pattern very similar to those profiles. Figure 2 shows that an increase in the heat dispersion coefficient causes the concentration boundary layer to narrow toward the wall. The mass transfer then increases at the same proportion. Here the mass transfer behavior with a varying Ra_ξ is similar to the purely diffusive case with changes on Le. This pattern could be anticipated, given the complete analogy between α and $\xi\nu$ in the two cases.

Table 4. Summary from the similarity solutions to flows of class 3

N	Ra_γ	$Nu_y(\xi/y)^{1/2}$	$Sh_y(\xi/y)^{1/2}$
0	1	0.377	0.424
	2	0.377	0.661
	4	0.377	1.014
	10	0.377	1.687
	100	0.377	5.558
	150	0.377	6.826
0.1	1	0.378	0.440
0.2	1	0.377	0.470
0.5	1	0.372	0.545
0.8	1	0.363	0.606
1	1	0.356	0.642
	2	0.324	0.948
	4	0.291	1.381
	10	0.256	2.230
	100	0.210	7.168
	150	0.206	8.788
2	1	0.326	0.794
	2	0.284	1.151
	4	0.244	1.655
	10	0.201	2.649
	100	0.149	8.453
	150	0.144	10.359
3	1	0.302	0.917
	2	0.255	1.318
	4	0.213	1.855
	10	0.170	3.005
	100	0.117	9.559
	150	0.112	11.712
4	1	0.282	1.023
	2	0.234	1.465
	4	0.191	2.088
	10	0.148	3.321
	100	0.097	10.546
	150	0.093	12.919
−1.1	1	1.508	0.298
−1.2	1	0.890	0.314
−1.5	1	0.529	0.369
−1.9	1	0.419	0.442
−2.0	1	0.405	0.460
−3.0	1	0.327	0.616
	2	0.254	0.838
−4.0	1	0.291	0.747
	2	0.224	1.030

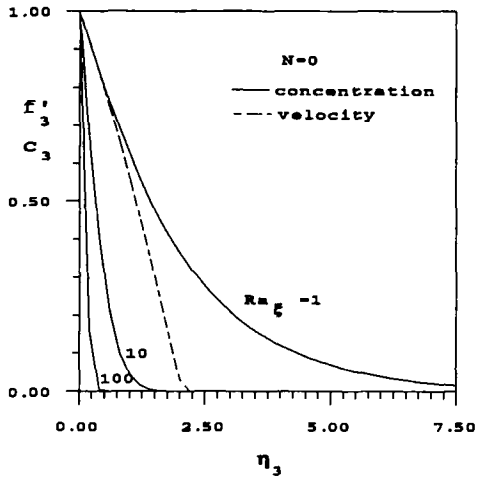

FIG. 2. Effect of thermal dispersion on fluid velocity and mass transfer for heat-transfer-driven flows of class 3.

Finally, regarding flows of class 4, the numerical integration of equation (27) was accomplished by using the smallest step size of all cases, $\Delta\eta = 5 \times 10^{-5}$. Strong relaxation parameters were needed in order to achieve convergence, mainly at the beginning of the calculation process. The reason for the increased degree of difficulty is the presence of higher order derivatives in all three governing equations. Going from class 1 to class 4 the difficulties build up as the number of derivatives brought into the system of coupled equations increases. In every case, both variables and derivatives were maintained as zero at the higher values of η. To reduce the computation time, the η_{max} value was leveled at 5.0, still rendering solutions insensitive to further increases in that value. Table 5 summarizes the results obtained for different values of N and dispersion ratio D_S. We consistently considered only cases with $\xi > \gamma$ ($D_S > 1$), in the range of practical interest. Taking into account the differences in the definitions of the similarity variables, the parallelism between Le in class 1 and D_S in class 4 may be recalled at this point to typify the influences of D_S on both heat and mass transfer. An increase in D_S causes the heat transfer rate to decrease in heat-

Table 5. Results of similarity solutions for dispersion-dominated flows

N	D_S	$Nu_y(\xi/y)^{1/2}$	$Sh_y(\xi/y)^{1/2}$
0	1	0.377	0.377
	2	0.377	0.611
	4	0.377	0.947
	8	0.377	1.420
	10	0.377	1.610
	100	0.377	5.477
1	1	0.377	0.377
	2	0.343	0.572
	4	0.309	0.851
	8	0.278	1.274
	10	0.270	1.401
	100	0.215	4.594
2	1	0.377	0.377
	2	0.332	0.559
	4	0.286	0.819
	8	0.244	0.184
	10	0.232	1.331
	100	0.159	4.308
3	1	0.377	0.377
	2	0.326	0.552
	4	0.274	0.802
	8	0.227	1.154
	10	0.213	1.295
	100	0.130	4.167
4	1	0.377	0.377
	2	0.323	0.548
	4	0.267	0.792
	8	0.217	1.136
	10	0.202	1.274
	100	0.113	4.084

transfer-driven flows. The mass transfer rate decreases in the same proportion in this case.

CONCLUDING REMARKS

Hydrodynamic dispersion in porous media affects both heat and mass transfer in natural convection flows. Departing from a general model to describe dispersivity in porous media, the present study addresses the dispersion effects in double-diffusive convection. Scale analysis is used to streamline the influences on the overall heat and mass fluxes along a straight vertical boundary. In the asymptotic limits, dispersion in boundary layer flows is described by simple form equations. Solutions of self-similarity are encountered for the governing equations. The numerical results obtained can be further used to check the scaling laws furnished by scale analysis. Figure 3 illustrates this verification for class 4 flows. According to Table 2

$$\left(\frac{Nu}{Sh}\right) \sim D_S^{-1/2}, \quad \text{for} \quad N \ll 1 \tag{36}$$

and

$$\left(\frac{Nu}{Sh}\right) \sim D_S^{-1}, \quad \text{for} \quad N \gg 1. \tag{37}$$

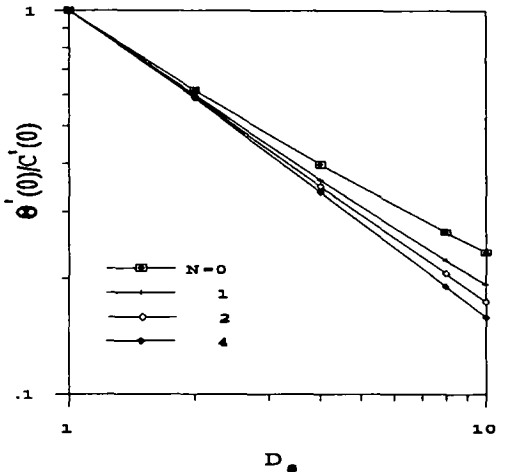

FIG. 3. Scaling relation for dispersion-dominated flows.

For $N = 0$ the slope in Fig. 3 is very close to $-1/2$, and as N increases the trend is to increase the curve slopes towards the unity exponent in the log–log plot.

REFERENCES

1. J. Bear, *Dynamics of Fluids in Porous Media*. American Elsevier, New York (1972).
2. G. I. Taylor, Dispersion of soluble matter in solvent flowing slowly through a table, *Proc. R. Soc.* **A219,** 186–203 (1953).
3. P. G. Saffman, Dispersion due to molecular diffusion and macroscopic mixing in flow through a network of capillaries, *J. Fluid Mech.* **7,** 194–208 (1960).
4. O. Trevisan and A. Bejan, Combined heat and mass transfer by natural convection in porous medium, *Adv. Heat Transfer* **20,** 315–349 (1990).
5. A. Bejan and K. R. Khairy, Heat and mass transfer by natural convection in a porous medium, *Int. J. Heat Mass Transfer* **28,** 909–918 (1985).
6. F. C. Lai and F. A. Kulacki, Coupled heat and mass transfer by natural convection from vertical surfaces in porous media, *Int. J. Heat Mass Transfer* **34,** 1189–1194 (1991).
7. T. K. Perkins and O. C. Johnston, A review of diffusion and dispersion in porous media, *Trans. AIME* **228,** (1963).
8. J. T. Hong and C. L. Tien, Analysis of thermal dispersion effect on vertical plate natural convection in porous media, *Int. J. Heat Mass Transfer* **30,** 143–150 (1987).
9. O. Kvernvold and P. Tyvand, Dispersion effects on thermal convection in porous media, *J. Fluid Mech.* **99,** 673–686 (1980).
10. O. A. Plumb, The effect of thermal dispersion on heat transfer in packed bed boundary layers, *ASME–JSME Joint Thermal Conf. Proc.*, Vol. 2, pp. 17–21 (1983).
11. J. A. Adams and D. F. Rogers, *Computer-aided Heat Transfer Analysis*. McGraw-Hill, New York (1973).
12. D. W. Marquardt, An algorithm for least squares estimation of nonlinear parameters, *J. Soc. Ind. Appl. Math.* **11,** 431–441 (1963).
13. R. S. Telles, Efeito da Dispersao Hidrodinamica na Conveccao Natural por Difusao Dupla em Meios Porosos. Ms. Thesis, UNICAMP, Campinas (1990).